Biofilm 9 (2025) 100251

Contents lists available at ScienceDirect

Biofilm

journal homepage: www.sciencedirect.com/journal/biofilm

Eicosapentaenoic acid as an antibiofilm agent disrupts mature biofilms of *Candida albicans*

Shuai Wang [a,1], Shiwang Xie [b,1], Tianmeng Li [a], Jun Liu [a], Peng Wang [a], Yu Wang [a], Li Gu [a], Dan Luo [b,**], Ming Wei [a,*]

[a] Department of Infectious Diseases and Clinical Microbiology, Beijing Institute of Respiratory Medicine and Beijing Chao-Yang Hospital, Capital Medical University, Beijing, China

[b] CAS Center for Excellence in Nanoscience, Beijing Key Laboratory of Micro-Nano Energy and Sensor, Beijing Institute of Nanoenergy and Nanosystems, Chinese Academy of Sciences, Beijing, China

ARTICLE INFO

Keywords:
Candida albicans
Candidemia
Biofilm
EPA
Transcriptome

ABSTRACT

The biofilm formation of *Candida albicans*, a major human fungal pathogen, represents a crucial virulence factor during candidiasis. Eicosapentaenoic acid (EPA), a polyunsaturated fatty acid, has emerged as a potential antibiofilm agent against *C. albicans*. Herein, we aim to investigate the antifungal effect of EPA (1 mM) on the mature biofilm of *C. albicans* and explore the underlying mechanism. Crystal violet and XTT assays showed that EPA exerted a strong inhibitory efficacy on preformed biofilms in *C. albicans*. Biofilm architecture and cell viability were observed using scanning electron microscopy and confocal laser scanning microscopy, indicating that EPA could block the yeast-to-hypha transition and damage the structure, thereby exhibiting antibiofilm activity. RNA sequencing analysis revealed that EPA treatment led to the downregulation of genes associated with hyphal formation and biofilm development. From the signaling pathway perspective, EPA regulated the *C. albicans* biofilms involving two signaling pathways, namely, Ras1-cAMP-PKA and Cek-MAPK pathways. Additionally, the EPA could effectively reduce the production of key messenger cAMP in the Ras1-cAMP-PKA pathway. Interestingly, in response to EPA, ergosterol biosynthesis-related genes were down-regulated, indicating EPA as antifungal agent might reduce the risk of developing drug resistance. The findings of this study highlight the potential of EPA as an alternative or adjunctive antibiofilm agent against *C. albicans*-related infections.

1. Introduction

Candidemia, an important nosocomial bloodstream infection associated with *Candida* spp., is most commonly caused by *C. albicans* [1]. It poses a significant threat worldwide, in terms of substantial mortality and high hospital costs [2–4]. The ability of *C. albicans* to persist as a biofilm on medical devices is a crucial virulence factor, which has been linked with poor clinical outcomes [5–7]. Biofilms formed by *C. albicans* are complex and structured microbial communities, consisting of yeast, hyphae, and pseudohyphae surrounded by a protective extracellular matrix [8]. These biofilms provide a robust defense mechanism, significantly enhancing tolerance against conventional antifungal agents and the host immune system [9]. Therefore, there is an urgent need for innovative antibiofilm treatment strategies to address this critical challenge.

Eicosapentaenoic acid (EPA), a member of the omega-3 polyunsaturated fatty acid family and one of the essential fatty acids for human health, has emerged as a promising antimicrobial agent [10]. Recent studies have reported that EPA can inhibit biofilm development by several microorganisms, including *Enterococcus faecium* [11], *Staphylococcus aureus* [12,13], *Staphylococcus epidermidis* [13], *Streptococcus mutans* [14], and some oral pathogenic bacteria [15,16].

Our previous research determined a significant antagonistic effect of EPA against *C. albicans* biofilms [17]. Notably, even mature biofilms, typically recalcitrant to antimicrobial agents, were effectively eradicated by 1 mM EPA. Furthermore, other studies have reported the

* Corresponding author.
** Corresponding author.
E-mail addresses: luodan@binn.cas.cn (D. Luo), weiming@bjmu.edu.cn (M. Wei).
[1] Contribute equally to the work.

https://doi.org/10.1016/j.bioflm.2024.100251
Received 16 October 2024; Received in revised form 15 December 2024; Accepted 29 December 2024
Available online 30 December 2024

antifungal properties of EPA on *C. albicans*. For example, Thibane et al. demonstrated that EPA could cause apoptosis in *C. albicans* biofilms, as indicated by a decrease in mitochondrial membrane potential and the occurrence of nuclear condensation and fragmentation [18]. Mokoena et al. discovered the EPA impacted *C. albicans* in *Caenorhabditis elegans* due to the inhibition of hyphal formation and stimulation of the host immune response [19]. However, the transcriptome-based biofilm-related changes remain to be elucidated.

A previous study suggested that medium-chain fatty acids mimicked the quorum-sensing molecule farnesol, and thus, caused physiological changes of fungal dimorphism, biofilm formation, and even cell death of *C. albicans* [20]. Farnesol, a by-product in the ergosterol biosynthetic process of *C. albicans*, has been shown to inhibit filamentation and biofilm formation primarily by regulating complex signaling pathways, one of the more well-studied interactions is the inhibitory role of farnesol on the cyclic AMP (cAMP) signaling pathway [21,22]. In addition, the mitogen-activated protein kinase (MAPK) signaling pathway is also a major regulatory pathway in controlling biofilm formation in *C. albicans* (mediated by the Cek1/2, Mkc1, or Hog 1 MAPK) [23,24]. It remains unknown whether EPA possesses antibiofilm activity against *C. albicans* potentially through analogous mechanisms as farnesol.

Therefore, this study aimed to elucidate the mechanism of EPA-mediated disruption of *C. albicans* biofilms using phenotypic and transcriptomic analysis. Delineating the mechanism of EPA-mediated disruption of *C. albicans* biofilms has the potential to inform the development of targeted therapeutic strategies for *Candida*-related biofilm infections.

2. Material and methods

2.1. Strains and growth conditions

This study used 31 clinical isolates of pre-characterized *C. albicans* with strong biofilm-forming ability from candidemia [17] and a reference strain *C. albicans* ATCC 90028. All *C. albicans* strains were routinely refreshed from the frozen stocks at −20 °C and inoculated at least twice onto Sabouraud Dextrose Agar (SDA) at 35 °C for 24 h before all experiments.

2.2. Reagents

EPA (20:5; ω-3) was purchased from Sigma-Aldrich (St. Louis, MO, USA). EPA was prepared as 2 M stock solutions in dimethyl sulfoxide (DMSO) and stored at −20 °C. Working solutions were prepared by diluting the stock with RPMI 1640 medium (Gibco, Thermo Fisher Scientific, Waltham, MA, USA). Our preliminary results show that DMSO at <0.1 % did not affect the growth or biofilm formation of *C. albicans*.

2.3. The minimum inhibitory concentration assay of EPA

The minimum inhibitory concentration (MIC) of EPA on planktonic cells of *C. albicans* was determined using the microdilution method. According to Clinical and Laboratory Standards Institute (CLSI) protocols [25], the initial concentration of the *C. albicans* suspension was adjusted to 1×10^3 CFU/mL in the RPMI 1640 medium. EPA was diluted in RPMI medium and tested at concentrations ranging from 0.125 mM to 1 mM. Following a 24 h incubation period at 35 °C, the MIC was determined visually as the lowest concentration at which there was a 50 % decrease in the growth of planktonic *C. albicans*. The assays were carried out in triplicate via three independent experiments.

2.4. Biofilm formation of C. albicans

The biofilms of *C. albicans* were prepared as described previously [17]. In brief, *C. albicans* cells were collected from overnight cultures and diluted to 1×10^5 CFU/mL with RPMI 1640 medium (Gibco, Thermo Fisher Scientific, Waltham, MA, USA). The *C. albicans* suspension was added into sterile 96-well round-bottomed polystyrene plates (Corning, NY, USA) of 200 μL each well, and the plates were incubated at 35 °C in an atmosphere of 5 % CO_2 for 24 h.

After incubation, the non-adherent cells were removed by washing gently with phosphate-buffered saline (PBS; pH 7.2) twice. Then, 200 μL of fresh RPMI 1640 medium with or without 1 mM EPA (Sigma-Aldrich; St. Louis, MO, USA) was added to the above microtiter plates to detect whether EPA impacts an established biofilm. RPMI 1640 medium supplemented with 0.1 % DMSO was used as a solvent control. After another incubation at 35 °C for 4 h or 24 h, the medium was aspirated, and non-adherent cells were removed by washing the biofilms with 200 μL of PBS twice.

2.5. Determination of the biomass of C. albicans biofilms

The *C. albicans* total biofilm mass was determined with the crystal violet (CV) assay previously described by Gulati et al. [26]. Briefly, the biofilms were fixed with 200 μL methanol for 15 min, stained with 200 μL crystal violet (0.2 %) for 20 min, and washed with distilled water. Then, the bound crystal violet was extracted with 200 μL of 33 % acetic acid. 150 μL of the obtained solutions were transferred to a new flat bottom 96-well plate, and the $OD_{630\ nm}$ values were measured using a Multiskan EX microplate photometer (Thermo Fisher Scientific, Waltham, MA, United States). The CV assays were performed in three independent biological replicates, each treatment in triplicates.

2.6. Determination of the metabolic activity of C. albicans biofilms

The metabolic activity was assessed with the XTT [2,3-bis-(2-methoxy-4-nitro-5-sulfophenyl)-2H-tetrazolium-5-carboxanilide] reduction assay as previously described by Manoharan et al. [27]. An XTT Cell Proliferation Kit II (Roche, Mannheim, Germany) was used according to the manufacturer's instructions. 200 μL of XTT solution was added to each well and incubated in the dark for 4 h at 35 °C. After incubation, 150 μL of the solutions were transferred to a new 96-well plate to measure the $OD_{450\ nm}$ values. The XTT assays were performed in three independent biological replicates, each treatment in triplicates.

2.7. Observations of the biofilm structure of C. albicans

The effect of EPA on the biofilm structure of *C. albicans* was examined by scanning electron microscopy (SEM) and confocal laser scanning microscopy (CLSM). Biofilms were formed on cover glass (Solarbio, Beijing, China) deposited in 6-well plates (Corning, NY, USA) (3 mL of cell suspension per well). After 24 h of incubation, the cover glass was washed twice with PBS and put in an empty microplate well. 3 mL of fresh RPMI 1640 medium with or without 1 mM EPA was added and incubated for 24 h at the same culture conditions.

For SEM, the biofilms were fixed in 2.5 % glutaraldehyde for 5 h at 4 °C, then were dehydrated in a sequential-graded ethanol (30 %, 50 %, 70 %, 80 %, 90 %, and 100 %), and then two times with 100 % ethanol for 15 min. Finally, the samples were sputter-coated with gold and observed with an SU8020 scanning electron microscope (Hitachi, Japan) [11].

For CLSM, the biofilms were stained with a live/dead viability kit (Invitrogen, CA, United States). The stain was prepared by diluting 3 μL of SYTO 9 and 3 μL of propidium iodide (PI) in 1.0 mL of filter-sterilized water. About 500 μL of staining solution was added to each biofilm sample. Samples were incubated for 30 min at room temperature in the dark. The biofilm architecture was then analyzed by a confocal laser scanning microscope (Leica TCS SP5, Germany). The excitation/emission was 488/498 nm for SYTO 9 and 535/617 nm for PI. Five random fields of view per experimental condition were imaged [28].

2.8. Transcriptomic analysis

2.8.1. RNA extraction

The total RNA was extracted from the EPA-treated and untreated biofilms of *C. albicans* isolate (ATCC 90028 and X27) using an RNAprep Pure Plant Kit (TIANGEN, Beijing, China) according to the manufacturer's instructions. The concentration and integrity of extracted RNA were assessed using a NanoDrop 2000 spectrophotometer (Thermo Scientific, USA) and Bioanalyzer 2100 system (Agilent Technologies, CA, USA).

2.8.2. RNA sequencing and analysis

RNA sequencing (RNA-Seq) was performed by Novogene Co., Ltd (Beijing, China) with the Illumina NovaSeq 6000 platform (Illumina, USA) and paired-end reads with an average length of 150 bp were obtained. The raw sequence data have been deposited into the SRA database under the accession number PRJNA1137062 (https://www.ncbi.nlm.nih.gov/sra/PRJNA1137062).

For RNA-seq analysis, raw paired-end reads were filtered using the Fastp program v0.19.7 under default parameters. Clean reads were mapped to the genome of *C. albicans* SC5314, retrieved from the Candida Genome Database (CGD) (www.candidagenome.org) using Hisat2 v2.0.5. Fragments per kilobase of transcript per million fragments mapped (FPKM) of each gene were calculated by FeatureCounts v1.5.0-p3. Gene expression analysis was performed using the DESeq2 R package (v1.20.0). The threshold of significantly differential expression genes (DEGs) between samples was the value of $|\mathrm{Log_2}\ (\text{fold change})| \geq 1$ and false discovery rate (FDR) < 0.05.

Gene ontology (GO) enrichment analysis and Kyoto Encyclopedia of Genes and Genomes (KEGG) pathway enrichment analysis of DEGs were performed with the ClusterProfiler (v3.8.1). Data represent three independent biological replicates for each condition.

2.9. Determination of intracellular cAMP levels

The intracellular cAMP concentration was measured with a Cyclic AMP Select ELISA kit (Cayman Chemical, United States) following the manufacturer's instructions. Briefly, the biofilms of *C. albicans* were washed twice with pre-cooled PBS. Then, biofilm cells were scraped from the plates and resuspended in 3 mL of 0.1 M HCl. Following sonication, the supernatants were collected by centrifugation at 1500*g* for 10 min and transferred to a fresh tube. Then, half of each sample was used to determine the total protein concentration with a Bradford 1 × dye reagent (Solarbio, Beijing, China), and the other half was used to measure the cAMP level with the ELISA kit. The intracellular cAMP concentrations were converted to picomoles per milligram of protein [29].

2.10. Statistical analysis

Statistical analysis was performed using the IBM SPSS Statistics 20.0 software program (IBM, Armonk, NY, USA). Data were expressed as means ± standard deviation (SD) of at least three independent experiments. A statistical comparison between the two groups was performed using the Student's *t*-test. A *P*-value <0.05 was considered statistically significant.

3. Results

3.1. Determination of MIC of EPA on planktonic cells of C. albicans

In this study, results showed the MICs of EPA against *C. albicans* were ≥1 mM, determined by the microdilution method to evaluate the antifungal activity of the EPA.

3.2. EPA affected preformed biofilm of C. albicans

The effect of EPA on the 24 h pre-formed biofilms biomass of 32 strains of *C. albicans* (a reference strain ATCC 90028 and 31 clinical isolates from candidemia) was evaluated. These strains have exhibited strong biofilm-forming abilities in our previous studies. The results showed EPA (1 mM) had a destructive effect on the 24 h pre-formed biofilms of 90.63 % (29/32) strains. The $OD_{630\ nm}$ values of *C. albicans* biofilms after EPA or RPMI 1640 medium treated 24 h were detected using the CV assay, as shown in Fig. 1A. The $OD_{630\ nm}$ for the EPA group (0.923 ± 0.273) was lower than that for the control group (1.096 ± 0.272). The difference was statistically significant ($P < 0.05$). Among the clinical isolates, EPA had the strongest impact on *C. albicans* X27, and the biofilm eradication rate was 46.02 %.

After it was established that EPA had a destructive effect on the biofilm of most *C. albicans* strains, *C. albicans* ATCC 90028 and X27 were selected for subsequent studies to clarify the mechanism. The biomass and metabolic activity of the biofilm were assessed at 4 h and 24 h post-treatment with either EPA or the control, using the CV and XTT assays, respectively (Fig. 1B and C). At 4 h, the biomass (0.794 ± 0.059 *vs.* 1.042 ± 0.025) and metabolic activity (2.253 ± 0.080 *vs.* 2.656 ± 0.094) of the biofilm decreased in the EPA group of *C. albicans* X27 compared with the control group, while the ATCC 90028 was not

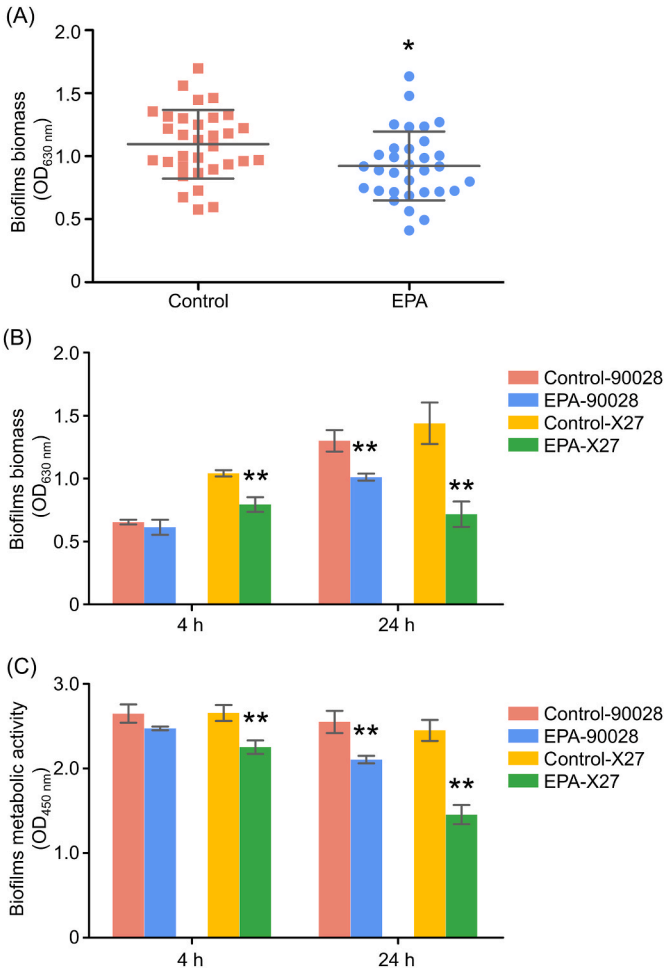

Fig. 1. The disruptive effect of EPA on 24 h pre-formed biofilms of *C. albicans*. (A) CV assay to assess the antibiofilm activity of EPA against 32 isolates of *C. albicans*. (B) Biofilms biomass of *C. albicans* ATCC 90028 and X27 treated by EPA after 4 h and 24 h. (C) Biofilms metabolic activity of *C. albicans* ATCC 90028 and X27 treated by EPA after 4 h and 24 h. Data are presented as means ± SD. **P* < 0.05, ***P* < 0.01, compared to the control group.

affected. By 24 h, the biomass and metabolic activity of both *C. albicans* ATCC 90028 (1.011 ± 0.028 *vs.* 1.300 ± 0.086; 2.105 ± 0.045 *vs.* 2.551 ± 0.132) and X27 (0.717 ± 0.101 *vs.* 1.439 ± 0.165; 1.455 ± 0.113 *vs.* 2.450 ± 0.124) biofilms had significantly decreased. The differences were statistically significant ($P < 0.01$).

3.3. EPA affected C. albicans morphology in biofilms

SEM provides a detailed visualization of the structure of *C. albicans* biofilms (Fig. 2). *C. albicans* biofilms treated with RPMI 1640 medium (control) formed dense and organized structures arranged in cellular multilayers, the biofilm consisted of mixtures of pseudohyphae/hyphae and a few yeast cells (Fig. 2A–C). In contrast, EPA-treated biofilms exhibited uneven distribution, mainly yeast-form cells (Fig. 2B–D).

CLSM was used to observe the cell viability of the biofilm treated with or without EPA. *C. albicans* cells with intact cell membranes emitted green fluorescence upon staining with SYTO 9, whereas cells with damaged membranes emitted red fluorescence upon staining with PI. As shown in Fig. 3, CLSM images displayed obvious changes in cell membrane integrity of *C. albicans* exposed to EPA compared with those of the control group, and the structural destruction in most of the biofilm was evident following EPA treatment.

3.4. Transcriptional response of C. albicans biofilms to EPA treatment

3.4.1. RNA-seq results quality analysis

The gene expression profile of *C. albicans* biofilms treated with 1 mM EPA for 24 h was compared with that treated with RPMI 1640 medium (control) by high-throughput RNA-seq. A comparative RNA-seq analysis was performed on two conditions (EPA and control) including two strains (ATCC 90028 and X27) with three independent biological replicates. A summary of reads obtained from each sample and their mapping to the reference genome (*C. albicans* SC5314) is given in Table 1. The Illumina sequencing of the 12 libraries generated 41–51 million raw reads per library. After quality control, 40–49 million clean reads were retained for each library. Approximately 98.71 % of the Q20 value and 96.32 % of the Q30 value were observed from RNA-seq data. Furthermore, more than 90 % of the clean reads could be uniquely mapped to the reference genome of *C. albicans*, indicating that the clean reads obtained were of high quality.

3.4.2. DEGs analysis

Principal-component analysis (PCA) was conducted to provide a pictorial representation of the transcriptomic similarities among biological replicates. As shown in Fig. 4A, all samples correlated well with biological replicates. The volcano plots were created with all the DEGs (Fig. 4B). The total DEGs in EPA-treated and untreated *C. albicans* biofilms were 438, of these, 205 and 233 genes were up- and down-regulated, respectively. A list of all significantly altered genes is provided in Table S1. The hierarchical clustering algorithm created a heat map (Fig. 4C). Three biological replicates in each group had similar gene expression patterns, and treatment groups differed significantly from the control.

In the analysis of the DEGs, about 44 % (191/438) of uncharacterized genes with unknown functions emerged. The characterized top 10 up- and down-regulated genes are listed in Table 2. Among the genes, 12 DEGs (*TNA1*, *EBP1*, *FGR41*, *ACE2*, *JEN2*, *SCW11*, *OYE22*, *CHT 3*, *HSP31*, *HHT21*, *ZRT2*, and *SSU1*) having roles in biofilm, 8 DEGs (*TNA1*, *FGR41*, *ACE2*, *SCW11*, *CFL11*, *PRA1*, *SSU1*, and *FGR2*) having roles in morphogenesis, and 5 DEGs (*BTA1*, *HGT9*, *GIT1*, *PGA50*, and *CWH8*) involving in other function.

3.4.3. GO enrichment analysis

To further understand the function of the DEGs, GO enrichment analysis was performed with the statistical DEGs. Based on GO enrichment analysis, the DEGs were assigned to 393 GO terms, including 204 biological processes, 65 cellular components, and 123 molecular functions. (Table S2). The top 10 GO enrichment terms in the 3 GO categories

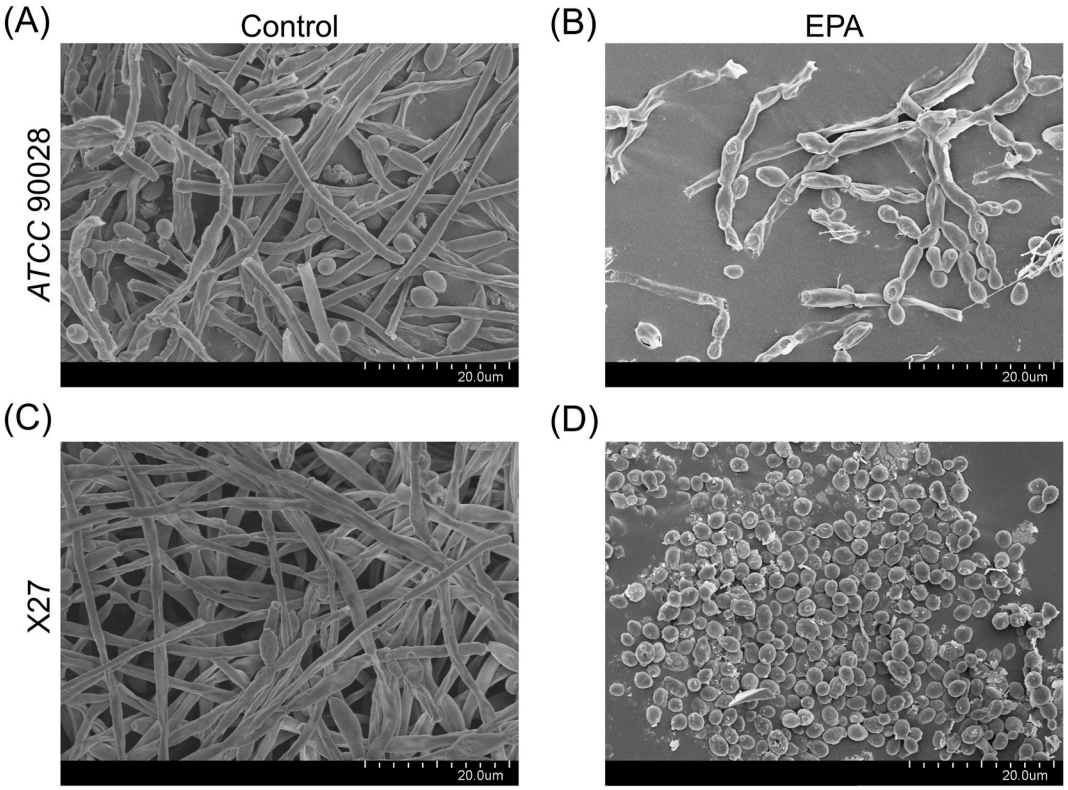

Fig. 2. Scanning electron microscopy (SEM) images of *C. albicans* biofilms treated with RPMI 1640 medium (control) or EPA. (A) Control group, *C. albicans* ATCC 90028. (B) EPA group, *C. albicans* ATCC 90028. (C) Control group, *C. albicans* X27. (D) EPA group, *C. albicans* X27. Scale bar = 20 μm.

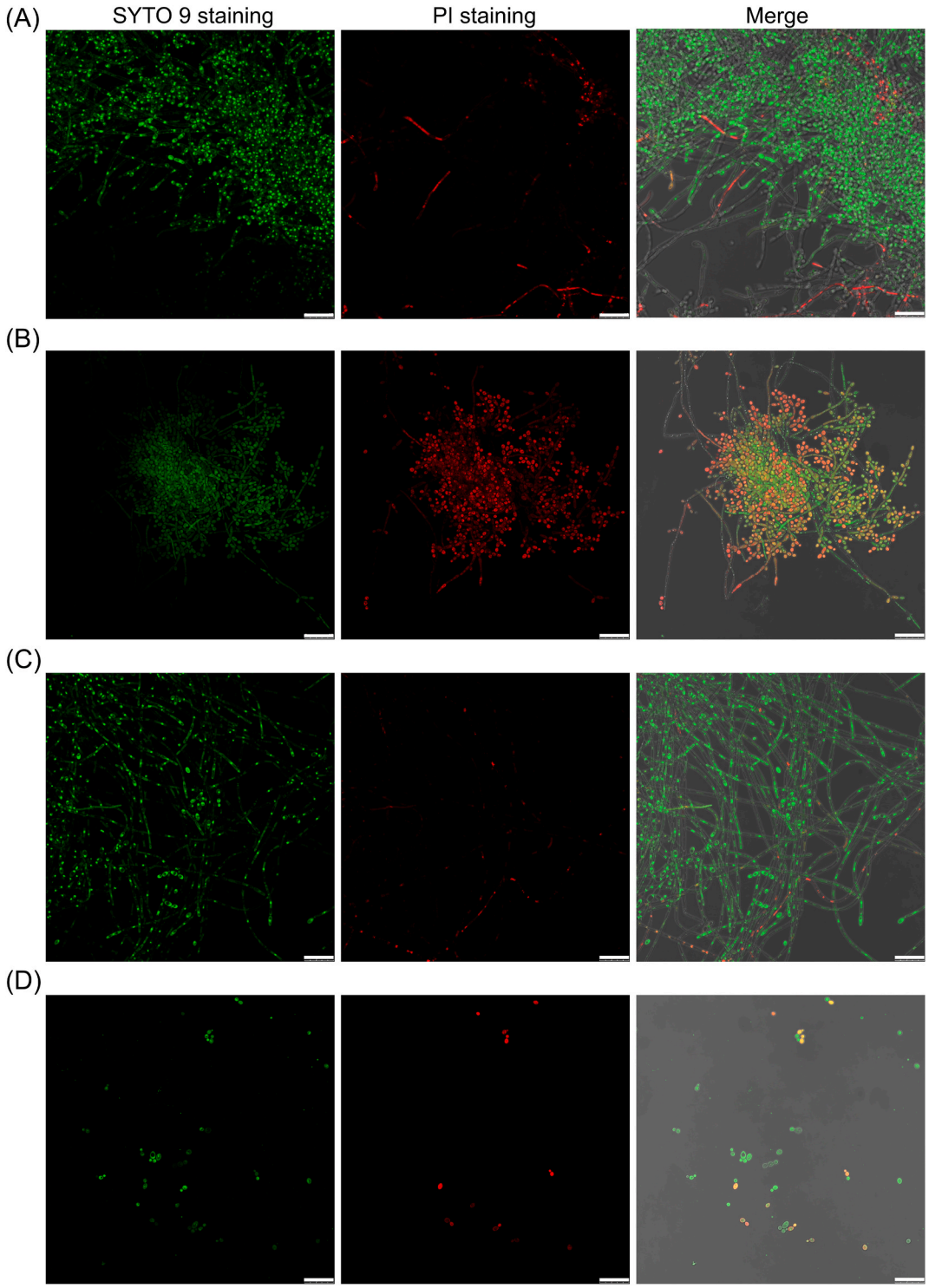

Fig. 3. Confocal laser scanning microscopy (CLSM) images of *C. albicans* biofilms treated with RPMI 1640 medium (control) or EPA. (A) Control group, *C. albicans* ATCC 90028. (B) EPA group, *C. albicans* ATCC 90028. (C) Control group, *C. albicans* X27. (D) EPA group, *C. albicans* X27. Green fluorescence denotes labeling with SYTO 9 for live cells, and red fluorescence denotes labeling with PI for dead cells. Scale bar = 25 μm. (For interpretation of the references to colour in this figure legend, the reader is referred to the Web version of this article.)

are shown in Fig. 5A. The statistically significant GO terms included 9 cellular components (GO:0032,993, GO:0000786, GO:0000785, GO:0044,815, GO:0016,020, GO:0016,021, GO:0031,224, GO:0044,427, and GO:0044,425), 10 molecular functions (GO:0048,037, GO:0046,982, GO:0005215, GO:0050,662, GO:0022,857, GO:0016,791, GO:0051,082, GO:0042,578, GO:0016,491, and GO:0019,842), and 2 biological processes (GO:0055,085 and GO:0055,114). The top-ranked cellular component was "protein-DNA complex" (7 up and 1 down), the top-ranked molecular function was "cofactor binding" (16 up and 9 down), and the top-ranked biological process was "transmembrane transport" (10 up and 29 down).

Table 1
Summary of quality control of RNA-seq results generated in the study.

Group	Sample name	Raw reads (bp)	Clean reads (bp)	Q20 (%)	Q30 (%)	GC (%)	Mapped read	Mapping ratio (%)
Control	C-90028-1	45,097,848	44,323,338	98.99	97.09	37.36	41,827,145	94.37
	C-90028-2	41,389,912	40,709,300	98.95	96.99	37.36	38,409,668	94.35
	C-90028-3	50,467,472	48,313,668	97.99	94.00	37.11	45,271,080	93.70
	C-X27-1	40,857,914	40,122,876	98.97	97.04	37.11	37,042,163	92.32
	C-X27-2	46,636,704	45,784,742	98.97	97.08	37.10	42,342,463	92.48
	C-X27-3	48,267,404	46,184,228	98.11	94.40	37.48	41,671,692	90.23
EPA	E−90028-1	46,980,998	45,757,454	98.71	96.48	37.41	43,440,221	94.94
	E−90028-2	47,358,956	46,592,240	98.77	96.60	37.52	44,125,478	94.71
	E−90028-3	46,548,132	45,796,242	98.74	96.54	36.96	43,203,889	94.34
	E-X27-1	44,805,798	44,212,514	98.77	96.58	37.58	41,204,463	93.20
	E-X27-2	43,859,334	43,322,624	98.75	96.52	37.45	40,301,513	93.03
	E-X27-3	42,673,636	42,126,644	98.75	96.53	37.24	38,907,463	92.36

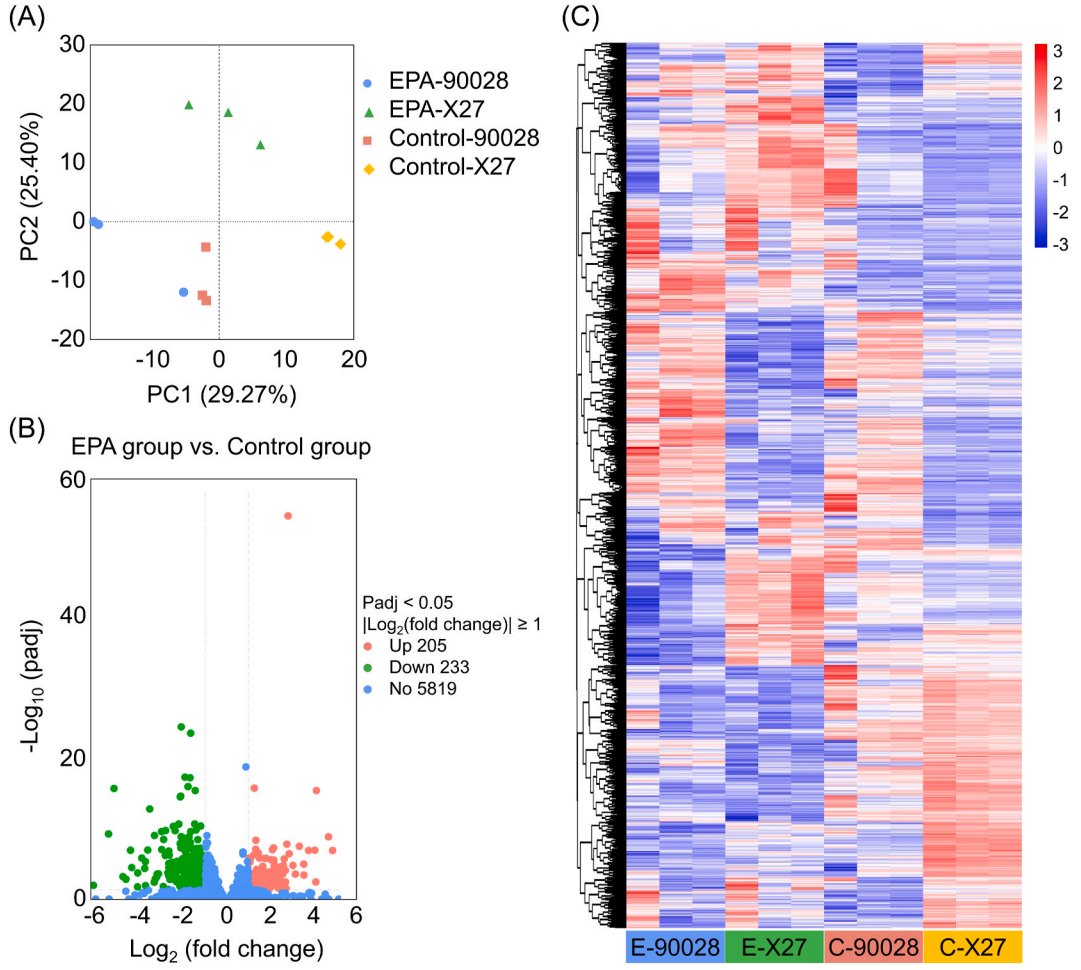

Fig. 4. Overall RNA-seq analysis of *C. albicans* biofilms in response to treatment with EPA. (A) Principal component analysis (PCA) of normalized RNA-seq read counts. (B) Volcano plots of DEGs for EPA group *vs.* control group. Red, green, and blue dots represent the up-regulated, down-regulated, and no-significant regulated genes. (C) Clustering heat map of expression levels for all identified DEGs. The transition from blue to red bands indicates increased gene expression levels. (For interpretation of the references to colour in this figure legend, the reader is referred to the Web version of this article.)

3.4.4. *KEGG pathway enrichment analysis*

In addition, the functions of DEGs were analyzed using the KEGG pathway enrichment analysis. 438 DEGs were enriched in 81 different pathways (Table S3), and the top 20 pathways are shown in Fig. 5B. These pathways mainly involve the metabolism (e.g., amino acid, carbohydrate, and lipid biosynthesis) and environmental information processing pathways. From the top 20 enriched KEGG pathways, the 12 terms of significantly enriched KEGG pathways were "Biosynthesis of secondary metabolites" (cal01110), "2-Oxocarboxylic acid metabolism" (cal01210), "Biosynthesis of amino acids" (cal01230), "Valine, leucine, and isoleucine biosynthesis" (cal00290), "Phenylalanine metabolism" (cal00360), "Tyrosine metabolism" (cal00350), "Butanoate metabolism" (cal00650), "Phenylalanine, tyrosine, and tryptophan biosynthesis" (cal00400), "Glyoxylate and dicarboxylate metabolism" (cal00630), and "Starch and sucrose metabolism" (cal00500).

Remarkably, by analyzing the heat map of gene expression related to the most enriched KEGG pathway "Biosynthesis of secondary metabolites" (Fig. 6), we found that three genes encoding key ergosterol biosynthesis enzymes, namely *ERG10*, *ERG12*, and *ERG13* were significantly down-regulated.

Table 2
Top 10 up/down-regulated characterized genes in EPA-treated *C. albicans* biofilms identified by RNA-seq.

Gene name	Log_2 (fold change) [a]	Description [b]
Up-regulated		
TNA1	4.67	Putative nicotinic acid transporter; detected at germ tube plasma membrane by mass spectrometry; rat catheter biofilm induced
EBP1	3.53	NADPH oxidoreductase; possible role in estrogen response; induced by oxidative, weak acid stress, NO, benomyl, GlcNAc; Cap 1, Mnl1 induced; Hap43-repressed; rat catheter biofilm induced
FGR41	3.33	Putative GPI-anchored adhesin-like protein involved in the regulation of covering cell wall glucan; transposon mutation affects filamentous growth; Spider biofilm repressed
ACE2	3.14	Transcription factor; regulates morphogenesis, cell separation, adherence, and virulence in mice; mutant is hyperfilamentous; rat catheter and Spider biofilm induced
JEN2	3.03	Dicarboxylic acid transporter; regulated by glucose repression; induced by Rgt1; rat catheter and Spider biofilm induced
SCW11	2.75	Cell wall protein; repressed in ace2 mutant; repressed in core caspofungin response; induced in high iron; possibly an essential gene; rat catheter and Spider biofilm repressed
OYE22	2.69	Putative NADPH dehydrogenase; rat catheter biofilm induced
CHT 3	2.63	Major chitinase; secreted; putative signal peptide; hyphal-repressed; farnesol upregulated in biofilm; regulated by Efg1p, Cyr1p, Ras1p
HSP31	2.63	Putative 30 kDa heat shock protein; repressed during the mating process; rat catheter biofilm induced
HHT21	2.59	Putative histone H3; amphotericin B repressed; regulated by Efg1, farnesol; Hap43-induced; rat catheter and Spider biofilm repressed
Down-regulated		
CFL11	−4.44	Superoxide-generating NADPH oxidase produces an extracellular burst of reactive oxygen species at growing cell tips during hyphal morphogenesis; regulated by Cdc42p
PRA1	−4.39	Cell surface protein that sequesters zinc from host tissue; enriched at hyphal tips; released extracellularly; binds to host complement regulators
BTA1	−3.65	Betaine lipid synthase
ZRT2	−3.35	Zinc transporter, essential for zinc uptake and acidic conditions tolerance; induced in oralpharyngeal candidiasis; Spider biofilm induced
HGT9	−3.34	Putative glucose transporter of the major facilitator superfamily; the *C. albicans* glucose transporter family comprises 20 members; 12 probable membrane-spanning segments
GIT1	−3.22	Glycerophosphoinositol permease; involved in utilization of glycerophosphoinositol as a phosphate source; Rim101-repressed; virulence-group-correlated expression
PGA50	−3.16	Putative GPI-anchored protein; adhesin-like protein
CWH8	−3.02	Putative dolichyl pyrophosphate phosphatase; ketoconazole-induced; expression is increased in a fluconazole-resistant isolate; Hap43p-induced gene
SSU1	−3.01	Protein similar to *S. cerevisiae* Ssu1 sulfite transport protein; Tn mutation affects filamentous growth; regulated by Gcn2 and Gcn4; Hap43-repressed; Spider and flow model biofilm induced
FGR2	−2.94	Protein similar to phosphate transporters; transposon mutation affects filamentous growth; expression is regulated upon white-opaque switching

[a] The Log_2 (fold change) was derived from RNA-seq results with an FDR of 0.05.
[b] As reported in the CGD database (http://www.candidagenome.org/).

3.5. EPA reduced the cAMP levels of *C. albicans* biofilms

It is known that the cAMP in *C. albicans* is the critical signaling molecule for the activation of the Ras1-cAMP-PKA pathway, therefore, we determined the production of intracellular cAMP levels in *C. albicans* biofilms treated with EPA at 24 h (Fig. 7). The results show that EPA can significantly reduce the production of cAMP ($P < 0.05$).

3.6. Effect of EPA on the gene expression of the related pathways of *C. albicans*

In addition, the expression levels of key genes in the Ras1-cAMP-PKA pathway were analyzed based on transcriptome data to explore further the effects of EPA in the cAMP signaling pathway (Fig. 8A). The expression of *RAS1*, *CYR1*, *TPK1*, *TPK2*, *BCY1*, and *TUP1* genes did not change significantly in EPA-treated group. The expression of transcription factor *EFG1* in this pathway was down-regulated and the expression of *NRG1* and *PDE2* were up-regulated. Fig. 8B showed EPA also could affect the expression levels of genes involved in the Cek-mediated MAPK pathway. The expression of *MSB2*, *OPY2*, and *CEK2* were down-regulated.

4. Discussion

Candida biofilms are complex and structured communities of microorganisms, that are notoriously difficult to eradicate due to their inherent resistance to conventional antifungal agents and host immune responses [30]. Therefore, there is a critical need for novel therapeutic approaches to effectively target biofilms, especially in disrupting mature biofilms.

This study demonstrated the potential of EPA, a polyunsaturated fatty acid, as an effective antagonist against biofilms formed by *C. albicans*. According to our previous research results, EPA at a concentration of 1 mM has a certain eradication activity on *C. albicans* biofilm, while EPA at a concentration of 0.01 or 0.1 mM has no eradication activity [17]. Therefore, in this study, we studied the effect of 1 mM EPA on the biofilm of *C. albicans*. Some articles indicated that a mature biofilm of *C. albicans* typically formed after 24–48 h [31–33]. Our previous study compared the biomass of *C. albicans* biofilm formation at different culture times, the results showed that compared with the biofilm biomass formed by *C. albicans* after 24 h, even though the biofilm biomass slightly increased at 48 h, the difference was not statistically significant ($P > 0.05$) (unpublished data). Therefore, we regarded 24 h pre-formed biofilms as mature biofilms in this study.

In this study, the results showed the biomass and metabolic activity of the biofilm decreased in the EPA-treated group compared with the control group (Fig. 1). Previous studies have also reported that EPA may have antibiofilm activities against pathogenic microorganisms [11–19].

We subsequently investigated the influence of EPA on the microstructure of *C. albicans* biofilms. SEM images (Fig. 2) clearly showed that EPA treatment led to substantial changes in the biofilm architecture. Specifically, the treated biofilms displayed fragmented and disorganized cell clusters, unlike the well-structured and compact layers observed in the control group. Additionally, individual *C. albicans* cells within the EPA-treated biofilms exhibited morphological transition. In *C. albicans*, the yeast-to-hypha transition is thought to play a crucial role in biofilm formation [34]. CLSM images (Fig. 3) revealed a marked reduction in biofilm biomass after 24 h of EPA exposure compared to the control group. These results indicate that EPA can regulate morphological transition, exhibiting antibiofilm activity. Similarly, Mokoena et al. showed that EPA could inhibit the hyphal formation of *C. albicans* in *Caenorhabditis elegans* [19].

Therefore, we further performed transcriptomic analyses to elucidate the potential molecular mechanisms underlying the antibiofilm action of EPA. The results of RNA-seq revealed that EPA treatment down-regulated the expression of adhesion-related genes (*DEF1*, *GWT1*,

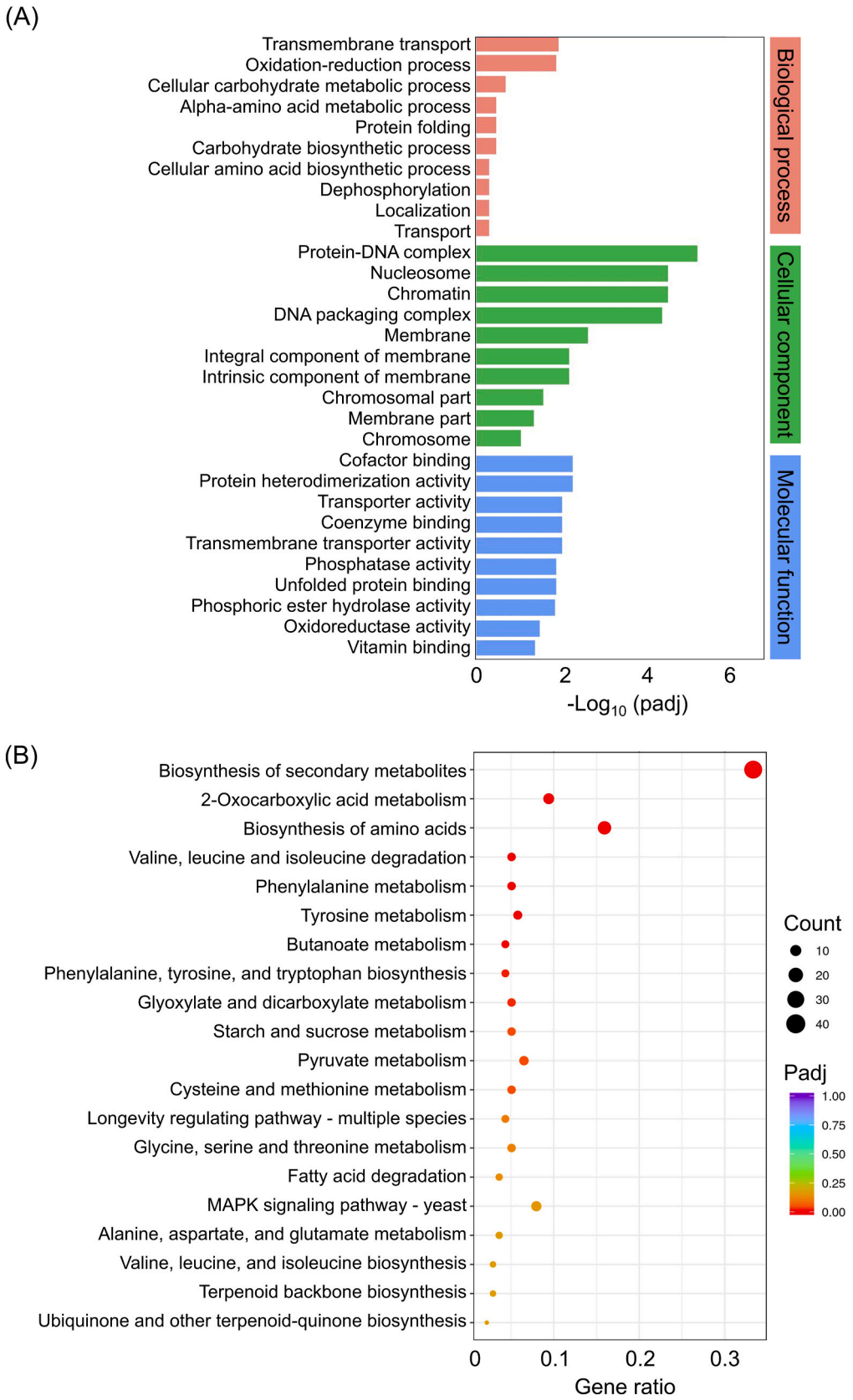

Fig. 5. Functional enrichment analysis of RNA-seq analysis in *C. albicans* biofilms in response to treatment with EPA. (A) Gene Ontology (GO) enrichment of DEGs between EPA and control group. Red, green, and blue bars represent biological processes, cellular components, and molecular functions, respectively. (B) Kyoto Encyclopedia of Gene and Genomes (KEGG) pathway enrichment of DEGs between EPA and control group. The size of the bubble means the number of different expression genes in this pathway. Low padj values are in red and high padj values are in blue, the size of the circle is proportional to the number of enriched genes. (For interpretation of the references to colour in this figure legend, the reader is referred to the Web version of this article.)

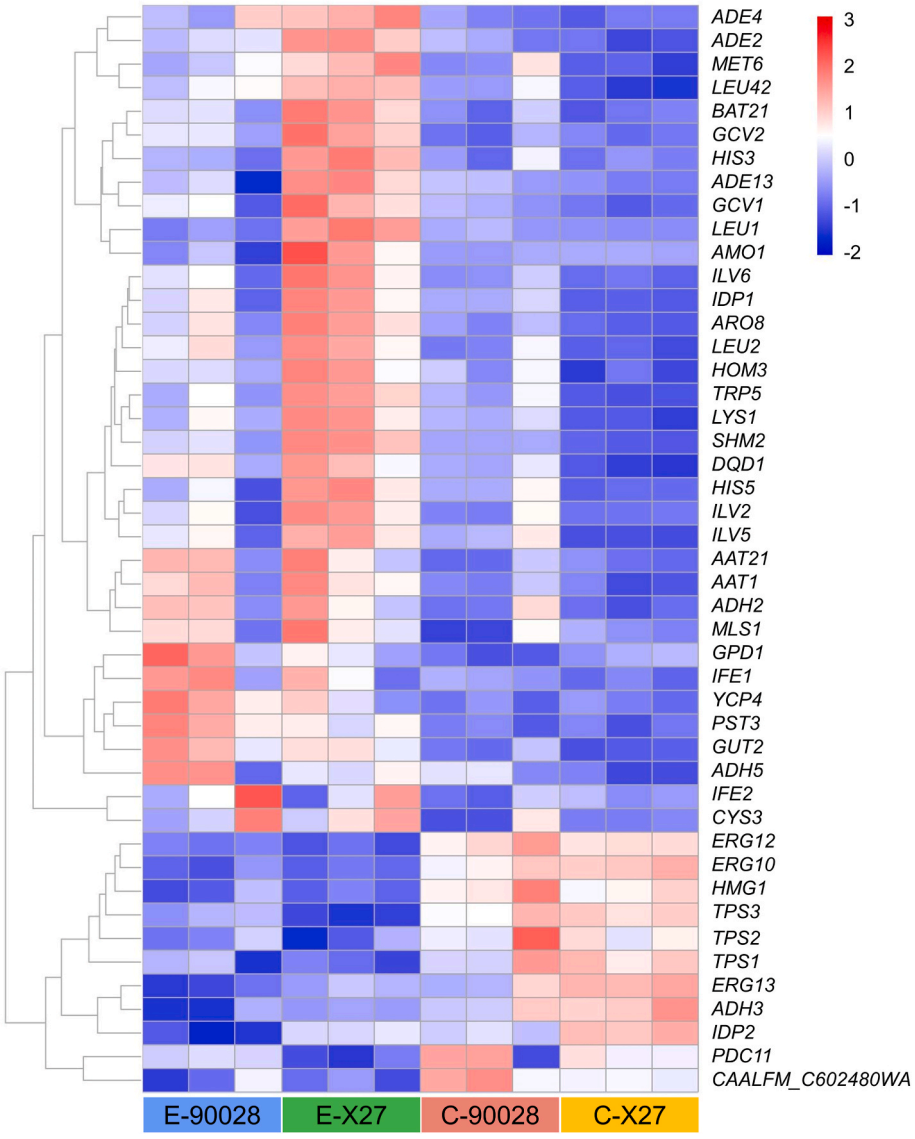

Fig. 6. Clustering heat map of expression levels of DEGs for biosynthesis of secondary metabolites pathway in KEGG pathways.

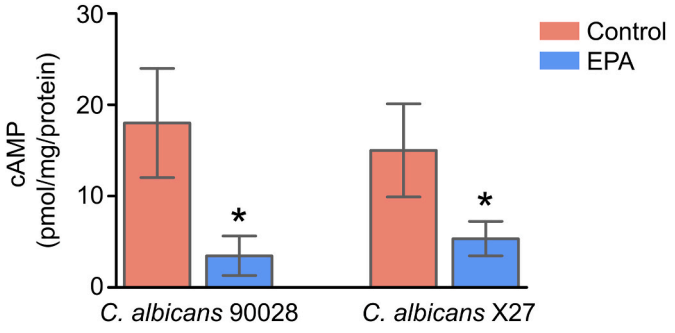

Fig. 7. Effect of EPA on the cAMP levels of *C. albicans* biofilms. Data are presented as means ± SD. *$P < 0.05$, compared to the control group.

HSL1, *PRA1*, *RFX2*, *SIT1*, *SUN41*, *TPS1*, and *TPS2*), hyphae-related genes (*CFL11*, *CSR1*, *DEF1*, *DFG5*, *ERG13*, *FAB1*, *FGR2*, *HSL1*, *MYO2*, *RFX2*, *SSU1*, *STE23*, *SUN41*, *TEM1*, *TEN1*, *TPS1*, and *VPS41*), and biofilm-related genes (*PRA1*, *CEK2*, *SWI4*, *SUN41*, *GWT1*, *MAC1*, and *RFX2*) (Table S1). Compared with the data from Mokoena et al. [19], which analyzed the influence of this EPA on the expression of *C. albicans* genes related to hyphal production in *C. elegans*, it is interesting that the *CSR1* gene was down-regulated in our study while up-regulated in theirs. Csr1 (also called Zap 1), is a zinc-specific transcription factor, that plays a key role in the hyphal formation of *C. albicans* [35]. This gene might be differentially expressed *in vitro* and *in vivo* after exposure to EPA. The specific functions of the gene during the infection of *C. albicans* in the presence of EPA requires further investigation.

From the signaling pathway perspective, EPA regulated the *C. albicans* biofilms involving two signaling pathways, Ras1-cAMP-PKA and Cek-MAPK pathways (Fig. 8). The Ras-cAMP-PKA signaling pathway triggers yeast-to-hypha transition in *C. albicans* [36]. The results showed that, in the presence of EPA, *PDE2* (phosphodiesterase 2 gene related to negative feedback regulation of hyphal formation) [37] and *NRG1* (key negative regulator gene of the yeast-to-hypha morphogenetic transition) [38] were slightly up-regulated. *EFG1* (master regulator gene of biofilm development) [39] was slightly down-regulated. Other major genes remained unchanged. Although EPA treatment might exert a minor influence on the Ras1-cAMP-PKA pathway, it could significantly reduce the level of cAMP (Fig. 7). The cAMP is crucial for activating the Ras1-cAMP-PKA signaling pathway. As a secondary messenger, cAMP binds to the regulatory subunits of PKA (Bcy1) and induces a conformational change that leads to dissociation and

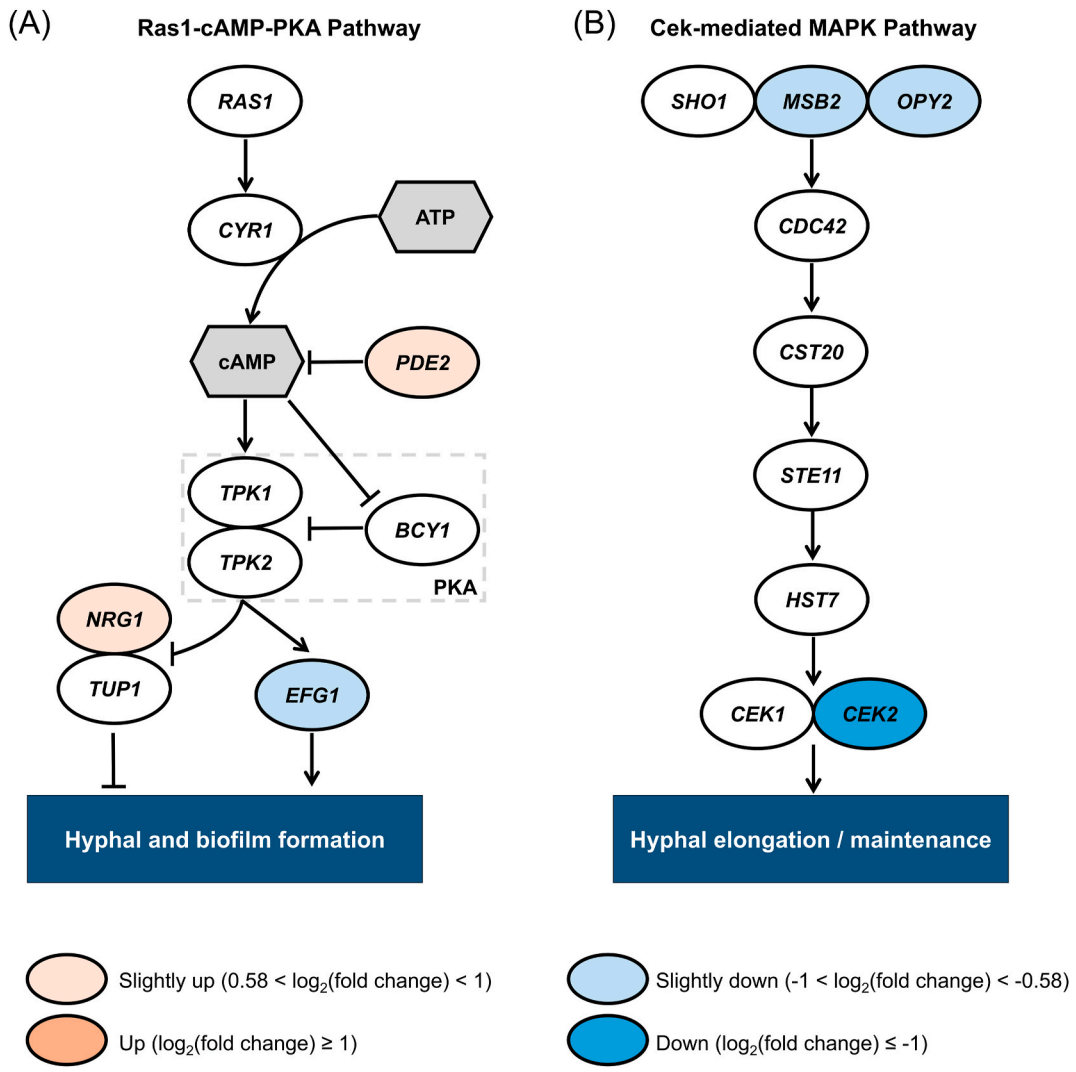

Fig. 8. Effect of EPA on (A) Ras1-cAMP-PKA and (B) Cek-mediated MAPK signaling pathways of *C. albicans*.

activation of the PKA catalytic subunits. This leads to activating the downstream transcription factor Efg1 [40]. Farnesol is a quorum sensing (QS) molecule synthesized by *C. albicans* acting as a negative regulator of morphogenesis mainly through the cAMP signaling pathway. Recently, various fatty acids were found to have antibiofilm activities and functionally similar to diffusible signal factors [41]. Therefore, we speculate that EPA may possess a function similar to that of a QS molecule. Regarding the Cek-MAPK signaling pathway, the gene expression level of *MSB2* (encoding mucin family adhesin-like protein) [42], *OPY2* (encoding transmembrane protein) [43], and *CEK2* (encoding MAPK) [44] were found to be down-regulated after EPA treatment. Besides, KEGG enrichment also showed that a large number of genes in the MAPK pathway were altered greatly in response to EPA (Fig. 5B). Cek2, as a member of the MAPK family, participates in multiple biological processes, including cell wall synthesis, morphogenesis, and responses to environmental stress [44]. During the elongation and maintenance of hyphae, Cek2 activates the expression of related genes by phosphorylating downstream effector molecules, thereby promoting the growth of hyphae. When the function of Cek2 is inhibited, hyphae cannot elongate and maintain normally, indirectly affecting the formation and stability of biofilms. These results suggested that EPA might inhibit the Ras1-cAMP-PKA and Cek-MAPK signaling pathways, resulting in an alternation mechanism underlying the yeast-to-hypha transition and biofilm development of *C. albicans*.

Furthermore, EPA exerted the antibiofilm effect also possible by targeting cell membrane components, such as interfering with the ergosterol biosynthesis. Ergosterol is an essential constituent of the fungal membrane for maintaining cell integrity, membrane fluidity, and cell metabolism [45]. It has been targeted for antifungal drug discovery. Exposed to EPA, ergosterol biosynthetic genes (*ERG10*, *ERG12*, *ERG13*, and *ERG28*) were significantly down-regulated. Since the increased expression levels of certain *ERG* genes can reduce the sensitivity to traditional antifungal drugs, such as fluconazole and amphotericin B, EPA may reduce the risk of developing drug resistance by inhibiting the expression of *ERG* genes [46–48].

While this study provides valuable insights into the antibiofilm mechanism of EPA against *C. albicans*, it has several limitations. This study primarily utilized *in vitro* biofilm models. The *in vitro* biofilm environment may not fully replicate the complex conditions of *in vivo* biofilm formation within a host. Moreover, although this study supplies several potential molecular explanations for the previously observed antibiofilm effects of EPA, further gene knockout studies in *vitro* and in *vivo* are required to verify that EPA regulates the pathways to disrupt the *C. albicans* biofilms.

In conclusion, the present study demonstrates that EPA exhibits antibiofilm activity against mature biofilms of *C. albicans* by inhibiting yeast-to-hypha transition. As far as we know, this is the first study highlighting the antibiofilm mechanism of EPA, which may be closely related to the Ras1-cAMP-PKA and Cek-MAPK pathways. Moreover, EPA significantly repressed the expression of ergosterol biosynthetic genes

and major metabolic pathways. These findings provide valuable insights into the potential application of EPA as an alternative or adjunctive therapeutic agent in managing *C. albicans* biofilm-related infections.

CRediT authorship contribution statement

Shuai Wang: Writing – original draft, Funding acquisition, Formal analysis. **Shiwang Xie:** Methodology, Investigation. **Tianmeng Li:** Investigation. **Jun Liu:** Validation. **Peng Wang:** Resources. **Yu Wang:** Visualization. **Li Gu:** Supervision. **Dan Luo:** Supervision, Conceptualization. **Ming Wei:** Writing – review & editing, Project administration, Conceptualization.

Funding

This work was supported by the National Natural Science Foundation of China (Grant No. 82302551); Beijing Natural Science Foundation (Grant No. 7234369); and the Reform and Development Program of Beijing Institute of Respiratory Medicine (Grant No. Ggyfz202425and Ggyfz202419).

Declaration of competing interest

The authors declare that they have no known competing financial interests or personal relationships that could have appeared to influence the work reported in this paper.

Acknowledgements

The authors would like to thank all members of the Department of Infectious Diseases and Clinical Microbiology staff at Beijing Chao-Yang Hospital (Beijing, China) for contributing to this work. We thank Dr. Zheng Liu for technical assistance with the CLSM imaging and analysis.

Appendix B. Supplementary data

Supplementary data to this article can be found online at https://doi.org/10.1016/j.bioflm.2024.100251.

Data availability

Data will be made available on request.

References

[1] Mccarty TP, White CM, Pappas PG. Candidemia and invasive candidiasis. Infect Dis Clin 2021;35(2):389–413.
[2] Tsay SV, Mu Y, Williams S, Epson E, Nadle J, Bamberg WM, et al. Burden of candidemia in the United States, 2017. Clin Infect Dis 2020;71(9):e449–53.
[3] Hou J, Deng J, Liu Y, Zhang W, Wu S, Liao Q, et al. Epidemiology, clinical characteristics, risk factors, and outcomes of candidemia in a large tertiary teaching hospital in western China: a retrospective 5-year study from 2016 to 2020. Antibiotics (Basel) 2022;11(6):788.
[4] Hoenigl M, Salmanton-Garcia J, Egger M, Gangneux JP, Bicanic T, Arikan-Akdagli S, et al. Guideline adherence and survival of patients with candidaemia in Europe: results from the ECMM *Candida* III multinational European observational cohort study. Lancet Infect Dis 2023;23(6):751–61.
[5] Rajendran R, Sherry L, Nile CJ, Sherriff A, Johnson EM, Hanson MF, et al. Biofilm formation is a risk factor for mortality in patients with *Candida albicans* bloodstream infection-Scotland, 2012-2013. Clin Microbiol Infect 2016;22(1):87–93.
[6] Tascini C, Sozio E, Corte L, Sbrana F, Scarparo C, Ripoli A, et al. The role of biofilm forming on mortality in patients with candidemia: a study derived from real world data. Inf Disp 2018;50(3):214–9.
[7] Vitalis E, Nagy F, Toth Z, Forgacs L, Bozo A, Kardos G, et al. *Candida* biofilm production is associated with higher mortality in patients with candidaemia. Mycoses 2020;63(4):352–60.
[8] Malinovska Z, Conkova E, Vaczi P. Biofilm formation in medically important *Candida* species. J Fungi (Basel) 2023;9(10):955.
[9] Lass-Florl C, Kanj SS, Govender NP, Thompson GR, Ostrosky-Zeichner L, Govrins MA. Invasive candidiasis. Nat Rev Dis Prim 2024;10(1):20.
[10] Das UN. Arachidonic acid and other unsaturated fatty acids and some of their metabolites function as endogenous antimicrobial molecules: a review. J Adv Res 2018;11:57–66.
[11] Wei M, Wang P, Li T, Wang Q, Su M, Gu L, et al. Antimicrobial and antibiofilm effects of essential fatty acids against clinically isolated vancomycin-resistant *Enterococcus faecium*. Front Cell Infect Microbiol 2023;13:1266674.
[12] Kim YG, Lee JH, Raorane CJ, Oh ST, Park JG, Lee J. Herring oil and omega fatty acids inhibit *Staphylococcus aureus* biofilm formation and virulence. Front Microbiol 2018;9:1241.
[13] Coraca-Huber DC, Steixner S, Wurm A, Nogler M. Antibacterial and anti-biofilm activity of omega-3 polyunsaturated fatty acids against periprosthetic joint infections-isolated multi-drug resistant strains. Biomedicines 2021;9(4):334.
[14] Sun M, Dong J, Xia Y, Shu R. Antibacterial activities of docosahexaenoic acid (DHA) and eicosapentaenoic acid (EPA) against planktonic and biofilm growing *Streptococcus mutans*. Microb Pathog 2017;107:212–8.
[15] Sun M, Zhou Z, Dong J, Zhang J, Xia Y, Shu R. Antibacterial and antibiofilm activities of docosahexaenoic acid (DHA) and eicosapentaenoic acid (EPA) against periodontopathic bacteria. Microb Pathog 2016;99:196–203.
[16] Ribeiro-Vidal H, Sanchez MC, Alonso-Espanol A, Figuero E, Ciudad MJ, Collado L, et al. Antimicrobial activity of EPA and DHA against oral pathogenic bacteria using an *in vitro* multi-species subgingival biofilm model. Nutrients 2020;12(9):2812.
[17] Wang S, Wang P, Liu J, Yang C, Wang Q, Su M, et al. Antibiofilm activity of essential fatty acids against *Candida albicans* from vulvovaginal candidiasis and bloodstream infections. Infect Drug Resist 2022;15:4181–93.
[18] Thibane VS, Ells R, Hugo A, Albertyn J, van Rensburg WJ, Van Wyk PW, et al. Polyunsaturated fatty acids cause apoptosis in *C. albicans* and *C. dubliniensis* biofilms. Biochim Biophys Acta 2012;1820(10):1463–8.
[19] Mokoena NZ, Steyn H, Hugo A, Dix-Peek T, Dickens C, Gcilitshana O, et al. Eicosapentaenoic acid influences the pathogenesis of *Candida albicans* in *Caenorhabditis elegans* via inhibition of hyphal formation and stimulation of the host immune response. Med Microbiol Immunol 2023;212(5):349–68.
[20] Lee JH, Kim YG, Khadke SK, Lee J. Antibiofilm and antifungal activities of medium-chain fatty acids against *Candida albicans* via mimicking of the quorum-sensing molecule farnesol. Microb Biotechnol 2021;14(4):1353–66.
[21] Zawrotniak M, Wojtalik K, Rapala-Kozik M. Farnesol, a quorum-sensing molecule of *Candida albicans* triggers the release of neutrophil extracellular traps. Cells 2019;8(12):1611.
[22] Rodrigues CF, Cernakova L. Farnesol and tyrosol: secondary metabolites with a crucial quorum-sensing role in *Candida* biofilm development. Genes 2020;11(4):444.
[23] Monge RA, Roman E, Nombela C, Pla J. The MAP kinase signal transduction network in *Candida albicans*. Microbiology (Read) 2006;152(Pt 4):905–12.
[24] Abdulghani M, Iram R, Chidrawar P, Bhosle K, Kazi R, Patil R, et al. Proteomic profile of *Candida albicans* biofilm. J Proteonomics 2022;265:104661.
[25] Wayne P, Clinical and Laboratory Standards Institute. Reference method for broth dilution antifungal susceptibility testing of yeasts. fourth ed. 2017. CLSI standard M27.
[26] Gulati M, Lohse MB, Ennis CL, Gonzalez RE, Perry AM, Bapat P, et al. *In vitro* culturing and screening of *Candida albicans* biofilms. Curr Protoc Microbiol 2018;50(1):e60.
[27] Manoharan RK, Lee JH, Kim YG, Lee J. Alizarin and chrysazin inhibit biofilm and hyphal formation by *Candida albicans*. Front Cell Infect Microbiol 2017;7:447.
[28] Mountcastle SE, Vyas N, Villapun VM, Cox SC, Jabbari S, Sammons RL, et al. Biofilm viability checker: an open-source tool for automated biofilm viability analysis from confocal microscopy images. NPJ Biofilms Microbiomes 2021;7(1):44.
[29] Liu C, Sun D, Liu J, Chen Y, Zhou X, Ru Y, et al. CAMP and c-di-GMP synergistically support biofilm maintenance through the direct interaction of their effectors. Nat Commun 2022;13(1):1493.
[30] Lohse MB, Gulati M, Johnson AD, Nobile CJ. Development and regulation of single- and multi-species *Candida albicans* biofilms. Nat Rev Microbiol 2017;16(1):19–31.
[31] Gulati M, Nobile CJ. *Candida albicans* biofilms: development, regulation, and molecular mechanisms. Microb Infect 2016;18(5):310–21.
[32] Mathe L, Van Dijck P. Recent insights into *Candida albicans* biofilm resistance mechanisms. Curr Genet 2013;59(4):251–64.
[33] Matsubara VH, Wang Y, Bandara HM, Mayer MP, Samaranayake LP. Probiotic lactobacilli inhibit early stages of *Candida albicans* biofilm development by reducing their growth, cell adhesion, and filamentation. Appl Microbiol Biotechnol 2016;100(14):6415–26.
[34] Iracane E, Vega-Estevez S, Buscaino A. On and off: epigenetic regulation of *C. albicans* morphological switches. Pathogens 2021;10(11):1463.
[35] Kim MJ, Kil M, Jung JH, Kim J. Roles of Zinc-responsive transcription factor Csr1 in filamentous growth of the pathogenic yeast *Candida albicans*. J Microbiol Biotechnol 2008;18(2):242–7.
[36] Hogan DA, Sundstrom P. The Ras/cAMP/PKA signaling pathway and virulence in *Candida albicans*. Future Microbiol 2009;4(10):1263–70.
[37] Wilson D, Tutulan-Cunita A, Jung W, Hauser NC, Hernandez R, Williamson T, et al. Deletion of the high-affinity cAMP phosphodiesterase encoded by PDE2 affects stress responses and virulence in *Candida albicans*. Mol Microbiol 2007;65(4):841–56.
[38] Murad AM, Leng P, Straffon M, Wishart J, Macaskill S, Maccallum D, et al. NRG1 represses yeast-hypha morphogenesis and hypha-specific gene expression in *Candida albicans*. EMBO J 2001;20(17):4742–52.
[39] Glazier VE. EFG1, everyone's favorite gene in *Candida albicans*: a comprehensive literature review. Front Cell Infect Microbiol 2022;12:855229.

[40] Lin CJ, Chen YL. Conserved and divergent functions of the cAMP/PKA signaling pathway in *Candida albicans* and *Candida tropicalis*. J Fungi (Basel) 2018;4(2):68.
[41] Kumar P, Lee JH, Beyenal H, Lee J. Fatty acids as antibiofilm and antivirulence agents. Trends Microbiol 2020;28(9):753–68.
[42] Roman E, Cottier F, Ernst JF, Pla J. Msb2 signaling mucin controls activation of Cek1 mitogen-activated protein kinase in *Candida albicans*. Eukaryot Cell 2009;8 (8):1235–49.
[43] Herrero DDC, Roman E, Diez C, Alonso-Monge R, Pla J. The transmembrane protein Opy2 mediates activation of the Cek1 MAP kinase in *Candida albicans*. Fungal Genet Biol 2013;50:21–32.
[44] Correia I, Roman E, Prieto D, Eisman B, Pla J. Complementary roles of the Cek1 and Cek2 MAP kinases in *Candida albicans* cell-wall biogenesis. Future Microbiol 2016;11(1):51–67.
[45] Lv QZ, Yan L, Jiang YY. The synthesis, regulation, and functions of sterols in *Candida albicans*: well-known but still lots to learn. Virulence 2016;7(6):649–59.
[46] Borecka-Melkusova S, Moran GP, Sullivan DJ, Kucharikova S, Chorvat DJ, Bujdakova H. The expression of genes involved in the ergosterol biosynthesis pathway in *Candida albicans* and *Candida dubliniensis* biofilms exposed to fluconazole. Mycoses 2009;52(2):118–28.
[47] Silva MC, Cardozo BCD, Diniz PF, Freitas FF, Fuzo CA, Santos PCTC, et al. Modulation of ERG genes expression in clinical isolates of *Candida tropicalis* susceptible and resistant to fluconazole and itraconazole. Mycopathologia 2020; 185(4):675–84.
[48] Fattouh N, Hdayed D, Geukgeuzian G, Tokajian S, Khalaf RA. Molecular mechanism of fluconazole resistance and pathogenicity attributes of Lebanese *Candida albicans* hospital isolates. Fungal Genet Biol 2021;153:103575.